



Brief Communications

Effects of entrainment and agglomeration of particles on combustion of nano-aluminum and water mixtures



Dilip Srinivas Sundaram, Vigor Yang*

School of Aerospace Engineering, Georgia Institute of Technology, Atlanta, GA 30332, USA

ARTICLE INFO

Article history:

Received 3 December 2013

Received in revised form 14 January 2014

Accepted 14 January 2014

Available online 6 February 2014

Keywords:

Nano-aluminum

Water

Combustion

Entrainment

Agglomeration

Flame propagation

ABSTRACT

The combustion of nano-aluminum and water mixtures is studied theoretically for a particle size of 80 nm and over a pressure range of 1–10 MPa. Emphasis is placed on the effects of entrainment and agglomeration of particles on the burning rate and its dependence on pressure. The flame thickness increases by a factor of ~ 10 , when particle entrainment is considered. This lowers the conductive heat flux at the ignition front, thereby reducing the burning rate. The pressure dependence of the burning rate is attributed to the changes in the burning time and velocity of particles with pressure. In the diffusion limit, the pressure exponent increases from 0 to 0.5, when the entrainment index increases from 0 to 1.0. A similar trend is observed in the kinetics-controlled regime, although the corresponding value exceeds the diffusion counterpart by 0.5. The kinetics-controlled model significantly over-predicts the burning rate and its pressure exponent, depending on the entrainment index. The present analysis suggests that nano-particles formed closely-packed agglomerates of diameter 3–5 μm , which may burn under diffusion-controlled conditions at high pressures.

© 2014 The Combustion Institute. Published by Elsevier Inc. All rights reserved

1. Introduction

Combustion of metal particles and water has been the focus of recent experimental studies [1–5]. The burning rate is inversely proportional to particle size [4,5] and has a pressure dependence of the form $r_b = ap^m$, with the exponent, m , in the range of 0.27–0.47 [4]. In our previous studies [6,7], a theoretical framework was established to predict the burning properties of nano-aluminum and water mixtures. The pressure dependence of the burning rate was attributed to the fact that the reaction rate is controlled by chemical kinetics or mass diffusion across the oxide layers of the particles. The oxide layer, however, may be fractured during ignition via core melting [8] and/or polymorphic phase transformations [9], and as a result, it is likely to offer negligible diffusion resistance. In order to capture the effect of particle size on the burning rate, a quadratic dependence of the burning time on particle size was assumed. This contradicts the hypothesis that nano-aluminum particles burn under kinetically-controlled conditions [10]. Furthermore, it does not explain why the pressure exponent in the burning-rate correlation varies with particle size and/or mixture consistency. The previous analysis also neglected convective motion of particles. In reality, the fluid velocity increases rap-

idly due to water vaporization and the particles can be transported by the gas flow, a phenomenon known as particle entrainment. The agglomeration of particles needs to be treated as well. The present study therefore attempts to address these two issues and shed light on their effects on the burning behaviors of nano-aluminum and water mixtures.

2. Theoretical framework

The analysis closely follows our previous approach [6,7], but is extended to include the convective motion and agglomeration of particles. The Maxwell–Eucken–Bruggeman model [11], which gives accurate predictions for all particle loading densities, has been used to calculate the effective thermal conductivity of the mixture. The particle entrainment effect is characterized by the particle velocity, u_p , expressed as

$$\frac{u_p}{r_b} = \left(\frac{\rho_{lw}}{\rho_{wv}} \right)^n, \quad (1)$$

where ρ is the density, r_b the burning rate and n is the entrainment index, which varies between zero (no entrainment) and unity (complete entrainment). The subscripts lw and wv refers to liquid water and water vapor, respectively. The expression for the heat flux at the ignition point ($x = 0$) is obtained by solving the energy equation in the reaction zone.

* Corresponding author. Fax: +1 404 894 2760.

E-mail address: vigor.yang@aerospace.gatech.edu (V. Yang).

$$\lambda \frac{dT}{dx} \Big|_R = \frac{\rho_m Q_r}{\tau_b k} + \frac{\lambda k}{\exp(kL) - 1} \left[(T_f - T_{ign}) - \frac{\rho_m Q_r L}{\lambda \tau_b k} \right], \quad (2)$$

$$L = r_b \tau_b \left(\frac{\rho_{lw}}{\rho_{wv}} \right)^n, \quad (3)$$

where λ is the thermal conductivity, T the temperature, x the spatial coordinate, Q_r the heat of reaction, τ_b the particle burning time, L the flame thickness, and k the ratio of the burning rate to thermal diffusivity. The subscripts R , m , ign , and f refer to the reaction zone, mixture, ignition, and flame, respectively. Note that the product kL is significantly lower than unity, especially for pressures representative of those in practical applications. Eq. (2) can, thus, be rewritten as

$$\lambda \frac{dT}{dx} \Big|_R = \frac{\lambda}{r_b \tau_b} \left(\frac{\rho_{wv}}{\rho_{lw}} \right)^n (T_f - T_{ign}). \quad (4)$$

By matching the energy fluxes in the preheat [7] and reaction zones at $x=0$, the following expression for the burning rate is obtained

$$r_b = \sqrt{\frac{\lambda}{\rho_m C_p} \frac{2C_p(T_f - T_{ign})}{2C_p(T_{ign} - T_u) + h_{fg}} \frac{1}{\tau_b} \left(\frac{\rho_{wv}}{\rho_{lw}} \right)^n}, \quad (5)$$

where C_p is the specific heat and h_{fg} the enthalpy of water vaporization. The expression bears close resemblance to that obtained in our previous work [7], except for the factor $(\rho_{wv}/\rho_{lw})^n$. Note that the particle-size effect originates from the burning time, whereas the pressure effect stems from the burning time and convective motion of particles.

3. Results and discussion

The theoretical framework discussed in Section 2 is employed to calculate the burning rate and flame structure of a stoichiometric 80 nm aluminum–water mixture. Figure 1 shows the burning rate and flame thickness as a function of the entrainment index at a pressure of 3.65 MPa. For the sake of consistency, the burning time of an individual particle is calculated using the correlation described in our previous work [7]. The burning rate decreases with increasing entrainment index, from a value of 1.9 cm/s at $n=0$ to 0.14 cm/s at $n=1$. Note that the flame thickness increases by a factor of ~ 10 due to particle entrainment. This lowers the conductive heat flux at the ignition point, thereby resulting in a slowly propagating flame.

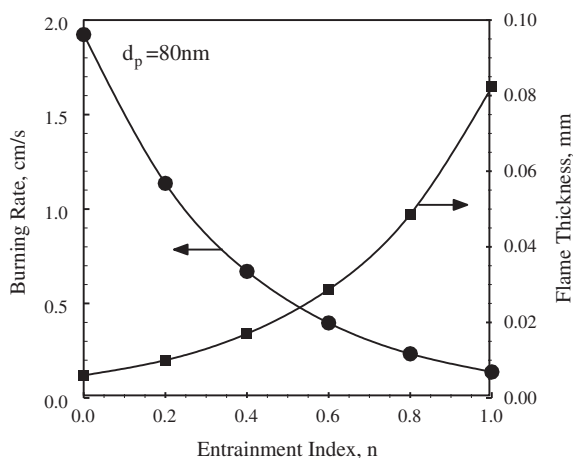


Fig. 1. Effect of entrainment index on burning rate and flame thickness of nano-aluminum and water mixtures for a particle size of 80 nm and pressure of 3.65 MPa.

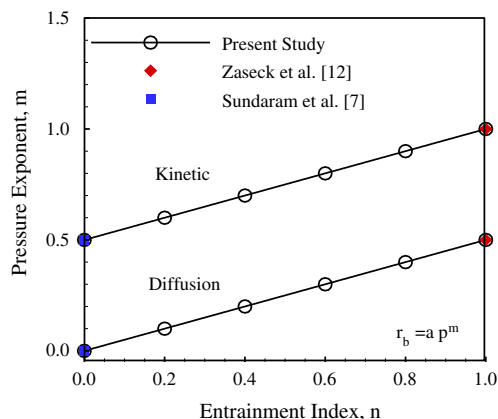


Fig. 2. Pressure exponent as a function of entrainment index for diffusion and kinetic controlled combustion mechanisms.

Figure 2 shows the burning-rate pressure exponent, m , for different entrainment indices, n . For diffusion-controlled combustion, entrainment causes the pressure exponent to increase from 0 to 0.5. A similar trend is observed in the kinetic regime, although the corresponding values exceed the diffusion counterparts by 0.5. The pressure exponents obtained by Zaseck et al. [12], shown in Fig. 2, are equal to those obtained in the present study for the case of complete particle entrainment. The value of m depends on mixture consistency, which can be altered by changing the particle size [13] or pH of water [14]. For example, the pressure exponent increases from 0.34 at pH = 6.16 to 0.68 at pH = 3.23, since the consistency changes from a paste to a fluid form. It is logical to expect loosely packed (or dispersed) particles to be more easily entrained by the gas flow. As a result, the differences in the measured pressure exponents can be attributed to the particle entrainment phenomenon.

The attractive forces can cause nano-particles to cluster and agglomerate, especially at higher particle loading densities [15]. The diameter of particle agglomerate can be calculated as [15]

$$d_{ag} = d_p \left(\frac{A}{4\pi\rho_p g z^2 d_p^2} \right)^{1/(D_0+2)}, \quad (6)$$

where d_{ag} is the diameter of the agglomerate, A the Hamaker constant and $z=4\text{ \AA}$ the minimum inter-molecular distance, g the acceleration due to gravity, ρ_p the particle density, and D_0 the fractal dimension. The Hamaker constant is about $1 \times 10^{-19} \text{ J}$ [16]. The fractal dimension is in the range of 2.5–3.0, which corresponds to closely-packed agglomerates [15]. For a particle size of 80 nm, the calculated diameter of the agglomerate is 3–6 μm . Figure 3 shows the effect of pressure on the burning rate of stoichiometric aluminum–water mixture containing 80 nm particles. For kinetically-controlled conditions, the particle burning-time correlation of Huang et al. [10] is employed. Two different burning-time pressure exponents, q , of 1.00 and 0.58 are considered. The former value is based on a theoretical study [17], while the latter is obtained from the experimental data of Bazyn et al. [18]. For the kinetics model, the predictions are greater than the experimental data by a factor as high as ten if particle entrainment is not considered. More accurate results are obtained, when the entrainment index, n , increases from 0.0 to 0.4. The resulting burning-rate pressure exponent, m , of 0.5 is, however, nearly twice the experimental value of 0.27. This is more so should a pressure exponent of unity be employed in the burning-time expression. For diffusion-controlled conditions, the burning time is calculated using Beckstead's correlation [19]. The diffusion model offers predictions that are in reasonably good

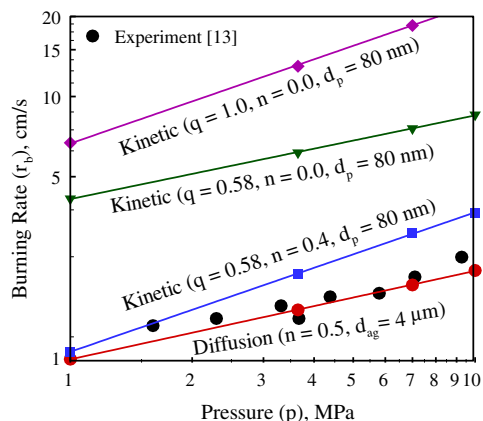


Fig. 3. Effect of pressure on the burning rate of stoichiometric aluminum–water mixture containing 80 nm particles.

agreement with experimental data when both entrainment and agglomeration of particles are considered. It is worth noting that the observed pressure dependence of the burning rate is more indicative of diffusion-controlled conditions. The inverse dependence of the burning rate on particle size is a result of the combustion of particle agglomerates as opposed to original particles. A predictive model of agglomeration of nano-aluminum particles in water vapor is therefore desired.

Acknowledgment

The authors would like to thank the Air Force Office of Scientific Research (AFOSR) for their sponsorship of this program under

Contract No. FA9550-13-1-0004. The support and encouragement provided by Dr. Mitat Birkan is greatly appreciated.

References

- [1] J.P. Foote, B.R. Thompson, J.T. Lineberry, in: G.D. Roy (Ed.), *Advances in Chemical Propulsion*, CRC Press, 2002, pp. 133–145.
- [2] E. Shafirovich, V. Diakov, A. Varma, *Combust. Flame* 144 (1–2) (2006) 415–418.
- [3] V.G. Ivanov, O.V. Gavriluk, O.V. Glazkov, M.N. Safronov, *Combust. Explos. Shock Waves* 36 (2000) 213–219.
- [4] G.A. Risha, S.F. Son, R.A. Yetter, V. Yang, B.C. Tappan, *Proc. Combust. Inst.* 31 (2007) 2029–2036.
- [5] M. Diwan, D. Hanna, E. Shafirovich, A. Varma, *Chem. Eng. Sci.* 65 (2010) 80–87.
- [6] D.S. Sundaram, V. Yang, T.L. Connell Jr., G.A. Risha, R.A. Yetter, *Proc. Combust. Inst.* 34 (2013) 2221–2228.
- [7] D.S. Sundaram, V. Yang, Y. Huang, G.A. Risha, R.A. Yetter, *Combust. Flame* 160 (2013) 2251–2259.
- [8] A. Rai, D. Lee, K. Park, M.R. Zachariah, *J. Phys. Chem. B* 108 (2004) 14793–14795.
- [9] M.A. Trunov, M. Schoenitz, E.L. Dreizin, *Combust. Theor. Modell.* 10 (2006) 603–623.
- [10] Y. Huang, G.A. Risha, V. Yang, R.A. Yetter, *Combust. Flame* 156 (2009) 5–13.
- [11] J. Wang, J.K. Carson, M.F. North, D.J. Cleland, *Int. J. Heat Mass Trans.* 49 (2006) 3075–3083.
- [12] C.R. Zaseck, S.F. Son, T.L. Pourpoint, *Combust. Flame* 160 (2013) 184–190.
- [13] G.A. Risha, J.L. Sabourin, V. Yang, R.A. Yetter, S.F. Son, B.C. Tappan, *Combust. Sci. Technol.* 180 (2008) 2127–2142.
- [14] D.E. Kittell, L.J. Groven, T.R. Sippel, T.L. Pourpoint, S.F. Son, *Combust. Sci. Technol.* 185 (2013) 817–834.
- [15] J. Valverde, A. Castellanos, *Chem. Eng. J.* 140 (2008) 296–304.
- [16] J.H. Masliyah, S. Bhattacharjee, *Electrokinetic and Colloid Transport Phenomena*, John Wiley & Sons, 2006.
- [17] R.A. Yetter, G.A. Risha, S.F. Son, *Proc. Combust. Inst.* 32 (2009) 1819–1838.
- [18] T. Bazyn, H. Krier, N. Glumac, *Combust. Flame* 145 (2006) 703–713.
- [19] M.W. Beckstead, *Combust. Expl. Shock Waves* 41 (2005) 533–546.